RSC Chemical Biology

ROYAL SOCIETY OF CHEMISTRY

COMMUNICATION

View Article Online
View Journal | View Issue

Cite this: *RSC Chem. Biol.*, 2025, **6**, 1716

Received 13th August 2025,
Accepted 2nd September 2025

DOI: 10.1039/d5cb00213c

rsc.li/rsc-chembio

Biosynthesis of sydonol reveals a new bisabolene cyclase and an unusual P450 aromatase

Peiyu Lu[ab] and Ling Liu *[ab]

In this work, the biosynthetic gene cluster and assembly line of sydonol were discovered and identified. As a result, and importantly, two unusual chemical conversions catalyzed by a new bisabolene cyclase and an unusual P450 aromatase were revealed: (1) cyclization of FPP to form 2, which involves a unique 1,5-proton transfer and a 1,7-hydride shift; and (2) aromatization of a bisabolene skeleton in the synthesis of 7.

Bisabolene-type sesquiterpenoids constitute an important family of natural products with diverse structural features and various bioactivities.[1–4] Their biosynthesis have been proposed to involve a common 1,6-closure bisabolyl cation intermediate, subsequently forming more complex sesquiterpenoid skeletons through multiple chemical transformations including hydride shift, alkyl shift, cyclization, or deprotonation reactions (Fig. 1 and Fig. S2).[5–8] For example, (1) the fungal UbiA-type transmembrane sesquiterpene cyclase (sesqui-TC) Fma-TC catalyzes 2,7-closure and C14 deprotonation of the bisabolyl cation to form β-*trans*-bergamotene,[9] a precursor of the human type 2 methionine aminopeptidase inhibitor fumagillin; and (2) the plant sesqui-TC ADS catalyzes successive 1,3-hydride shift, 1,10-closure and C12 deprotonation reactions of the bisabolyl cation to generate amorphadiene,[10,11] a backbone of the well-known artemisinin.

Of the isolated bisabolene-type sesquiterpenoids, a subclass of compounds from *Aspergillus sydowii* or *A. versicolor*,[12–15] for instance sydonol (**1**), (Fig. 1) especially caught our attention. Compared to the previously reported bisabolene-type sesquiterpenoids, these compounds have unusual structural features: mainly (1) a saturated terminal pendent isopentane group, with the mechanism of formation of these compounds significantly different from the typical cyclization mechanism of known bisabolene cyclases;[16–21] and (2) a C5 hydroxyl benzene ring, with unusual oxidation reactions perhaps involved in the transformation of the bisabolene skeleton.

Based on these distinctive structural features, the biosynthetic pathway of compound **1** was then investigated. We sequenced the genome of the sydonol-producing strain *A. sydowii* LF51 and analyzed its possible terpene synthase gene clusters. A total of six terpene gene clusters were identified in *A. sydowii* LF51, with the cluster in scaffold 14 (namely *syd* cluster, Fig. 2a. GeneBank: PX243221) appearing to be the candidate for the synthesis of **1**. This inference is based on a phylogenetic analysis showing the TC Syd1 to be closely related to the known clade of bisabolene cyclases (Fig. S3). In addition to *syd1*, two cytochrome P450 genes (*syd2* and *syd3*) and a short-chain dehydrogenase/reductase gene (SDR, *syd4*) were identified in the *syd* cluster. These three genes were here proposed to be responsible for the subsequent oxidation tailoring steps.

To confirm the function of Syd1, its intron-free cDNA was cloned under the ADH2 promoter and transferred into the *Saccharomyces cerevisiae* RC01.[22] After three days of fermentation followed by extraction with *n*-hexane, a compound (**2**) with a molecular weight (MW) of 204 was detected in *S.c-sdy1* in a

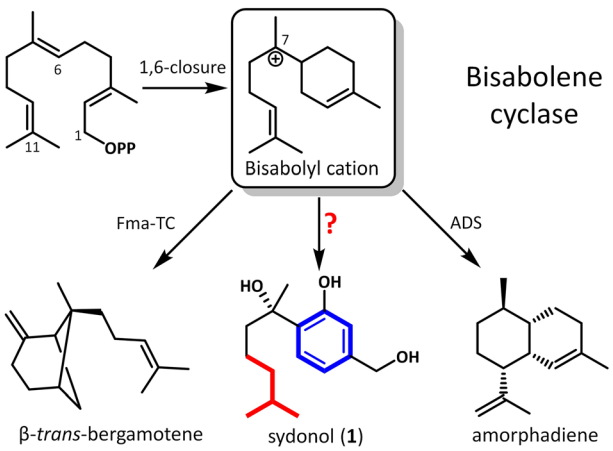

Fig. 1 Representative examples of bisabolene cyclases.

[a] *State Key Laboratory of Microbial Diversity and Innovative Utilization, Institute of Microbiology, Chinese Academy of Sciences, Beijing 100101, China. E-mail: liul@im.ac.cn*
[b] *University of Chinese Academy of Sciences, Beijing 100049, China*

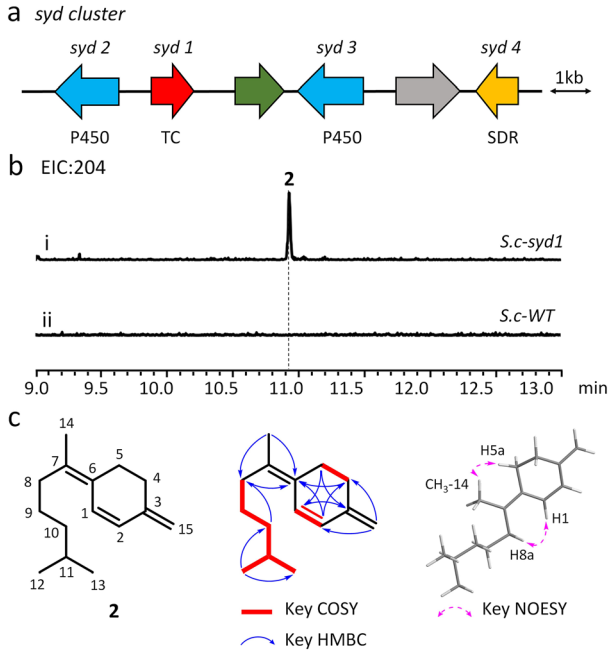

Fig. 2 Functional confirmation of *syd1*. (a) Organization and proposed function of *syd* gene cluster (green: transcription factor, grey: MFS-type transporter). (b) GC-MS analysis showing *syd1* having catalyzed the formation of **2**. (c) Structure determination of **2**.

GC-MS analysis (Fig. 2bi and ii). Subsequently, compound **2** was purified from the large-scale fermentations of *S.c-sdy1* and its structure was further confirmed in an NMR analysis (Fig. S29–S35 and Table S7). A structural analysis (Fig. 2c) confirmed that compound **2** possesses a bisabolene skeleton, notably featuring an unusual arrangement of three conjugated double bonds—with Δ^6 in the *Z* configuration—and a saturated terminal pendant isopentane unit.

To solidify our understanding of the function of Syd1 in the formation of **2**, we expressed and purified Syd1 from *E. coli* (Fig. S4). When Syd1 was incubated with FPP and Mg^{2+}, the formation of **2** was detected (Fig. 3ai and iv). This result clearly confirmed Syd1 to be a new bisabolene cyclase, with it alone catalyzing the cyclization of FPP to give **2**, and with the most important transformation during this cyclization process being the formation of the saturated C10/C11 bond.

To further investigate the Syd1 cyclization mechanism, we performed an *in vitro* assay of Syd1 in D_2O buffer. GC-MS analysis showed no ^2H atom incorporated into **2** (Fig. 3aii), indicating that no deprotonation-reprotonation process occurred when the saturated C10/C11 bond formed. Alternatively, the migration of protons might have occurred during Syd1-catalyzed cyclization, possibly through an intramolecular hydride shift, *e.g.*, an unusual 1,7-hydride shift (from H1 to H11).

Based on this hypothesis, we first chemically synthesized the deuterated 1,1-$^2H_2$-FPP (see SI) and used it as a substrate to incubate with Syd1. GC-MS analysis showed that the MW of this deuterated **2** was 2 Da greater than that of unlabelled **2** (Fig. 3aiii), suggesting that the 1,1-$^2H_2$ of FPP was kept in **2**, and a hydride shift indeed occurred. Following its preparation form the *in vitro* large-scale bioconversion of **2**, the deuterated compound **2** was purified and its structure was confirmed (Fig. S36 and S37). By comparing the results for the deuterated and unlabelled **2**, migration of the 1-^2H in FPP from C1 to C11 was discovered, specifically from the disappearance of the H-1 signal and the singlet pattern of H-2 in the deuterated **2**, as well as the disappearance of HMBC correlations between H1 and C1 as well as H11 and C11 (Fig. 3b). Based on this observation, a Syd1 cyclization mechanism was proposed, in which 1,5-proton transfer and 1,7-hydride shift occurred after the formation of a 1,6-closure bisabolyl cation intermediate, resulting in the formation of another cationic intermediate, which was eventually deprotonated to generate **2** (Fig. 3e).

We next investigated the key residues for Syd1. (1) Analysis of its active-site sequence showed the typical motif 2 (N_{225}DXXSXXXE$_{233}$) of Syd1 to be intact, but motif 1 (DD/EXXD) changed to D_{99}EEYM$_{103}$. The alanine-scanning mutations confirmed the importance of D99 and E233, as their variants significantly reduced and almost abolished the activity of Syd1, respectively (Fig. 3d). (2) Further molecular docking of Syd1 to the proposed 1,6-closure bisabolyl cation intermediate and the mutation experiments indicated a possible involvement of 11 residues (I73, I96, F156, R182, G186, F187, I221, D222, Y294, R304 and Y305) in the Syd1-catalyzed cyclization process (Fig. 3c). Notably, the I73A/R182K/G186A/D222A/Y305A variants produced farnesol and R182K/F187A/D222A variants produced a new compound, namely **3** (Fig. 3d and e, Fig. S38–S44 and Table S8), which suggested a key role for these residues in initiating and controlling the Syb1 cyclization process, especially for D222/F187 in the formation of a C3-cation–π interaction before its final deprotonation process.

Confirming the unique Syd1 cyclization mechanism facilitated our investigation of the function of the remaining genes in the *syd* cluster. (1) When the intron-free *syd2–4* genes were introduced into *S.c-sdy1*, the resulting transformant *S.c-sdy1234* could produce **1** (Fig. 4ai and ii). (2) Elimination of *sdy4* did not affect the production of **1** by *S.c-sdy123*, indicative of *sdy4* not being involved in the synthesis of **1** (Fig. 4aiii). (3) *S.c-sdy12* did not produce **1**, but three compounds (**5–7**) accumulated (Fig. 4aiv). Subsequent isolation and structural determinations using HRMS and NMR analyses (Fig. 4b, Fig. S8–S11, S45–S73 and Tables S9–S12) showed that compounds **5–7** all contained the intact C5-hydroxyl–substituted benzene ring. However, at the C7 position, **5** attached an ethanolamine moiety through a C–N bond, **6a**/**6b** had attached a cysteine moiety through a C–S bond and **7** had attached a hydroxyl group through a C–O bond.

Syd3 was concluded from these results to be responsible for the inert C15 hydroxylation on **7** to generate **1**, with this hydroxylation being the last step during the synthesis of **1** (Fig. 4c). Importantly, these results revealed Syd2 to be an unusual P450, catalyzing a series of complex transformations on **2** to synthesize **5–7** *in vivo*. This identifies Syd2 as the first aromatase to convert a bisabolene skeleton into a C5-hydroxyl–substituted benzene ring. Based on this information, we proposed a plausible mechanism for a multifunctional CYP450-mediated aromatization process (Fig. 4c). The initial

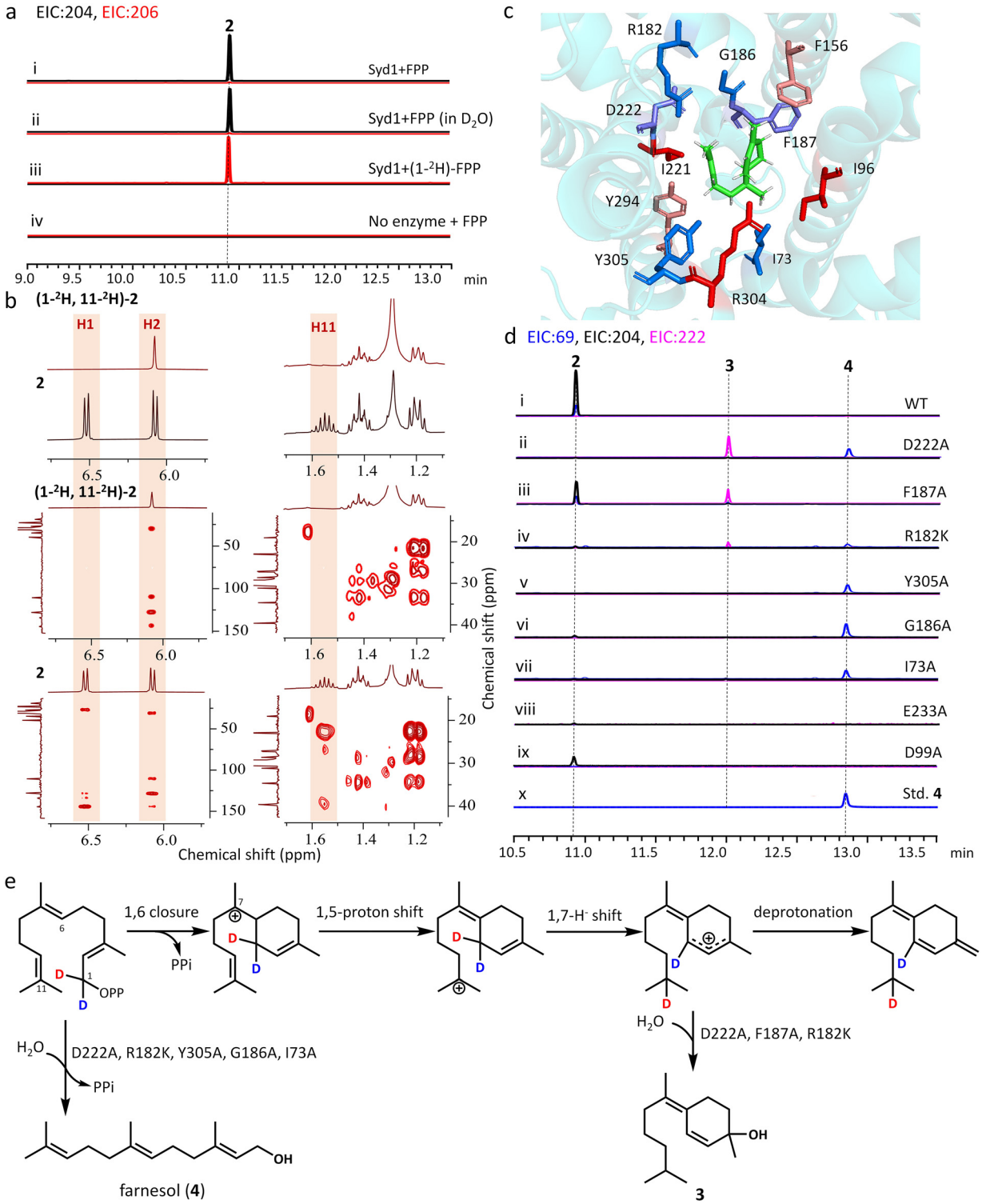

Fig. 3 Mechanistic evidence for Syd1 catalysis of the formation of **2**. (a) GC-MS analysis of the enzymatic reactions catalyzed by Syd1. (b) Comparative ^{1}H NMR and HMBC spectral analyses of **2** and (1-^{2}H, 11-^{2}H)-**2**. (c) Key residue interactions in Syd1-bisabolyl cation docking model. (d) GC-MS analysis of the enzymatic reactions catalyzed by Syd1 variants. EIC: *m/z* 69 represents the most prominent characteristic ion fragment of farnesol, EIC *m/z* 204 and EIC *m/z* 222 correspond to the molecular ions of **2** and **3**, respectively. (e) Proposed mechanisms for the cyclization of FPP to **2** and the enzyme-variants–catalyzed conversion of FPP to **3** and **4**.

monooxygenation of **2** occurs *via* a P450-mediated radical rebound mechanism through radical A· to yield B, which then undergoes hydrogen atom abstraction and radical rebound at the opposing face of the cyclohexene ring to generate geminal

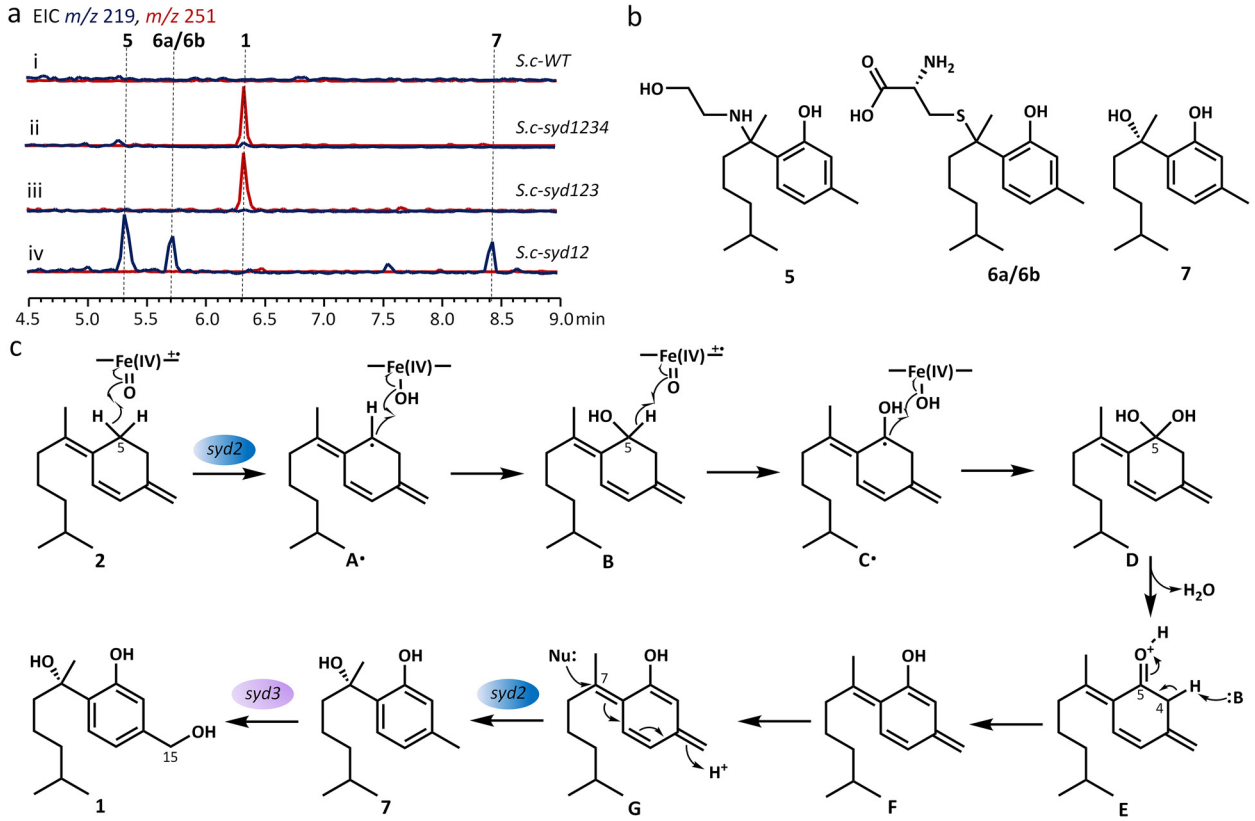

Fig. 4 Functional characterization of Syd2 and Syd3. (a) LC-MS analysis of gene combinations revealed the essential roles of *syd2* and *syd3* in the biosynthesis of **1**. (b) Structures of compounds **5**, **6a**/**6b** and **7**. (c) Proposed mechanisms for the Syd2-catalyzed conversion of **2** to **5**, **6a**/**6b** and **7** and biosynthetic pathway producing **1**.

diol D, with subsequent dehydration generating a ketone intermediate that tautomerizes to enol F. The enol F then undergoes double-bond isomerism *via* nucleophilic addition mediated by H_2O, endogenous ethanolamine or cysteine to afford **5**, **6a**/**6b** and **7**, respectively.[23–25] Note that only **1** was detected in *S.c-sdy123*, *i.e.*, the corresponding C15-hydroxyl products of **5** and **6** were not observed; thus, **5** and **6** should be considered to be shunt products.

Conclusions

In summary, we achieved a discovery of the biosynthetic gene cluster and the demonstration of a three-gene cassette for the synthesis of sydonol. The sydonol assembly line involves two unusual chemical conversions: (1) cyclization of FPP to form **2**, which includes a unique 1,5-proton transfer and a 1,7-hydride shift; and (2) aromatization of the bisabolene skeleton in the synthesis of **7**. Our work not only reveals an aromatase P450 enzyme catalyzing previously unidentified sesquiterpenoid aromatization reactions but also provides valuable biocatalytic tools for the structural diversification of terpenoids.

Conflicts of interest

There are no conflicts to declare.

Data availability

All relevant data generated or analyzed during this study are within the manuscript and its SI. Supplementary information: Experimental procedures, chromatograms, tables listing strains, plasmids and PCR primers, as well as spectroscopic data. See DOI: **https://doi.org/10.1039/d5cb00213c**.

Acknowledgements

This study was financially supported by grants from the National Key Research and Development Program of China (2022YFC2303100) and the National Natural Science Foundation of China (32472320 and 32022002).

Notes and references

1 H. Z. Shu, C. Peng, L. Bu, L. Guo, F. Liu and L. Xiong, *Phytochemistry*, 2021, **192**, 112927.
2 C. S. Li, L. T. Liu, L. Yang, J. Li and X. Dong, *Front. Chem.*, 2022, **10**, 881767.
3 Z. Li, Y. Yang, C. Chen, L. Lin, C. Tang and Y. Ye, *J. Nat. Prod.*, 2023, **86**, 1550–1563.
4 Y. Q. Guo, G. X. Wu, C. Peng, Y. Q. Fan, L. Li, F. Liu and L. Xiong, *Molecules*, 2023, **28**, 2704.

5 D. Tholl, F. Chen, J. Petri, J. Gershenzon and E. Pichersky, *Plant J.*, 2005, **42**, 757–771.
6 Y. J. Hong and D. J. Tantillo, *J. Am. Chem. Soc.*, 2009, **131**, 7999–8015.
7 Y. J. Hong and D. J. Tantillo, *J. Am. Chem. Soc.*, 2014, **136**, 2450–2463.
8 M. Dixit, M. Weitman, J. Gao and D. T. Major, *ACS Catal.*, 2017, **7**, 812–818.
9 H. C. Lin, Y. H. Chooi, S. Dhingra, W. Xu, A. M. Calvo and Y. Tang, *J. Am. Chem. Soc.*, 2013, **135**, 4616–4619.
10 D. Lubertozzi and J. D. Keasling, *J. Ind. Microbiol. Biotechnol.*, 2008, **35**, 1191–1198.
11 Y. J. Hong and D. J. Tantillo, *Chem. Sci.*, 2010, **1**, 609–614.
12 X. D. Li, X. Li, X. M. Li, X. L. Yin and B. G. Wang, *Nat. Prod. Res.*, 2021, **35**, 4265–4271.
13 M. Elsbaey, C. Tanaka and T. Miyamoto, *Phytochem. Lett.*, 2019, **32**, 70–76.
14 Y. Q. Jiang, C. Y. Cui, C. M. Chen, N. Wang, H. Liao, Q. Li, L. Mao, N. J. Ding, J. B. Kang, J. B. Kang, J. J. Zhou, H. C. Zhu, Y. J. Lai, Z. P. Wang, Q. Zhou and Y. H. Zhang, *Chem. Biodivers*, 2023, **20**, e202301047.
15 X. Yang, H. J. Yu, J. W. Ren, L. Cai, L. J. Xu and L. Ling, *J. Fungi*, 2023, **9**, 347.
16 F. Lopez-Gallego, S. A. Agger, D. Abate-Pella, M. D. Distefano and C. Schmidt-Dannert, *ChemBioChem*, 2010, **11**, 1093–1106.
17 L. Lauterbach, A. Hou and J. S. Dickschat, *Chem. – Eur. J.*, 2021, **27**, 7923–7929.
18 J. S. Dickschat, N. L. Brock, C. A. Citron and B. Tudzynski, *ChemBioChem*, 2011, **12**, 2088–2095.
19 M. Dixit, M. Weitman, J. Gao and D. T. Major, *ACS Catal.*, 2018, **8**, 1371–1375.
20 L. Lauterbach and J. S. Dickschat, *Org. Biomol. Chem.*, 2020, **18**, 4547–4550.
21 T. T. Lou, A. Li, H. C. Xu, J. F. Pan, B. Y. Xing, R. B. Eu, J. S. Dickschat, D. H. Tang and M. Ma, *J. Am. Chem. Soc.*, 2023, **145**, 8474–8485.
22 M. C. Tang, H. C. Lin, D. H. Li, Y. Zou, J. Li, W. Xu, P. A. Cacho, M. E. Hillenmeyer, N. K. Garg and Y. Tang, *J. Am. Chem. Soc.*, 2015, **137**, 13724–13727.
23 J. Brzywczy, R. Natorff, M. Sieńko and A. Paszewski, *Res. Microbiol.*, 2007, **158**, 428–436.
24 Y. Tao, D. D. Zheng, W. Zou, T. Guo, G. J. Liao and W. Zhou, *Eur. J. Med. Chem.*, 2024, **271**, 116461.
25 M. P. Torrens-Spence, R. V. Guggenberg, M. Lazear, H. Z. Ding and J. Y. Li, *BMC Plant. Biol.*, 2014, **14**, 247.